A global geography of synchrony for terrestrial vegetation

Emma J. Defriez[1]

Daniel C. Reuman[2,3]

Article type: Research article

Affiliations: [1] Imperial College London, Silwood Park, Buckhurst Road, Ascot, Berkshire, SL5 7PY, UK, e.defriez11@imperial.ac.uk; [2] Department of Ecology and Evolutionary Biology and Kansas Biological Survey, University of Kansas, Lawrence, Kansas, 66047, USA, reuman@ku.edu; [3] Laboratory of Populations, Rockefeller University, 1230 York Ave, New York, New York, 10065, USA.

Correspondence: Daniel C Reuman, Department of Ecology and Evolutionary Biology and Kansas Biological Survey, Higuchi Hall, University of Kansas, Lawrence, KS, 66047, reuman@ku.edu.

Keywords: Enhanced vegetation index, remote sensing, spatial modeling, cospectrum, geography, primary production

Running title: geography of synchrony in vegetation

Number of words in abstract: 274

Number of words in paper, Introduction through Biosketch: 5685

Number of references: 49

1 ABSTRACT

Aim: Previous work demonstrated a pronounced geography of synchrony for marine phytoplankton, and used that geography to infer statistical environmental determinants of synchrony. Here we determine if terrestrial vegetation (measured by the Enhanced Vegetation Index, EVI) also shows a geography of synchrony, and we infer determinants of EVI synchrony. As vegetation is the basis of the terrestrial food web, changes in spatio-temporal vegetation dynamics may have major consequences.

Location: The land.

Time period: 2001-2014.

Major taxa: Plants.

Methods: Synchrony in terrestrial vegetation is mapped globally. Spatial statistics and model selection are used to identify main statistical determinants of synchrony and of geographic patterns in synchrony.

Results: The first main result is that there is a pronounced and previously unrecognized geography of synchrony for terrestrial vegetation. Some areas such as the Sahara and Southern Africa exhibited nearly perfect synchrony, whereas other areas such as the Pacific coast of South America showed very little synchrony. Spatial modeling provided the second main result that synchrony in temperature and precipitation were major determinants of synchrony in EVI, supporting the presences of dual global Moran effects. These effects depended on the timescales on which

synchrony was assessed, providing our third main result: synchrony of EVI and its geography are timescale specific.

Main conclusions: To our knowledge, this study is the first to document the geography of synchrony in terrestrial vegetation. We showed geographic variation in synchrony is pronounced. We used geographic patterns to identify determinants of synchrony. This study is one of very few studies to demonstrate two separate synchronous environmental variables driving synchrony simultaneously. The geography of synchrony is apparently a major phenomenon that has been little explored.

2 INTRODUCTION

Understanding the dynamics of terrestrial vegetation biomass and production is both an interesting and important topic: vegetation is constantly changing over a range of temporal and spatial scales (Ichii *et al.*, 2002; Zhu *et al.*, 2016); and it is a key component of the global carbon cycle (Beer *et al.*, 2010; Wieder *et al.*, 2015) that is tightly coupled with climate because it directly affects land-atmosphere heat and moisture fluxes (Meir *et al.*, 2006). Of course vegetation is also the base of the terrestrial food web and hence the dynamics of vegetation biomass or production is implicated in essentially every area of pure and applied ecology. Therefore, changes in details of vegetation dynamics, including spatio-temporal aspects of those dynamics, may have far reaching consequences.

One incompletely understood aspect of spatio-temporal vegetation dynamics is their spatial synchrony. Spatial synchrony is the phenomenon whereby geographically separate population time series (or, in this context, vegetation biomass or production time series) fluctuate partly in

unison. Spatial synchrony has been observed even in populations separated by hundreds or thousands of kilometers (Post & Forchhammer, 2004; Liebhold *et al.*, 2004), across a very wide variety of taxa including protists, insects, fish, birds, mammals, and many others (Hanski & Woiwod, 1993; Myers *et al.*, 1997; Liebhold *et al.*, 2004). One of the primary mechanisms that has been cited to account for synchrony is the presence of spatially synchronized environmental factors which drive population dynamics, thereby inducing synchrony in the populations. This is known as the Moran effect (Moran, 1953). The Moran effect is one of the main causes of synchrony (Lande *et al.*, 1999; Liebhold *et al.*, 2004), but historically it was difficult to convincingly show that Moran effects operate in specific scenarios and to identify the environmental drivers (Liebhold *et al.*, 2004; Abbott, 2007). This was partly because the historically most common statistical descriptors of synchrony can show similar patterns for Moran effects and for other causes of synchrony (Ranta *et al.*, 1999; Abbott, 2007).

We previously mapped global geographic variation in patterns of synchrony in ocean phytoplankton (Defriez & Reuman, In review). We thereby provided evidence that a Moran effect, operating through synchronized sea surface temperatures or through synchrony of an environmental variable highly correlated with sea surface temperature such as nutrient availability, and possibly acting through complex oceanographic mechanisms, is a major driver of phytoplankton synchrony globally. The main goal of the present study is to apply the same statistical techniques to map the geography of synchrony in terrestrial vegetation, and then to infer determinants of synchrony in vegetation. Temperature and precipitation are two important climatic variables affecting productivity (Nemani *et al.*, 2015; Clinton *et al.*, 2014); and Koenig (2002) found synchrony in both of these factors over large spatial scales (up to 5000km). Vegetation dynamics may be similarly synchronized. Shetakova *et al.* (2016) investigated tree growth in two contrasting forest biomes and found that large scale synchrony responded to

climate warming. But the detailed geography of synchrony in terrestrial vegetation and the extent to which that geography reflects geographic patterns of synchrony in temperature and precipitation variables are unknown.

Multiple methods have been used to describe patterns of spatial synchrony, ranging from standard methods based on correlation coefficients (Hanski & Woiwod, 1993; Bjørnstad & Falck, 2001) to spectral and wavelet methods (Grenfell *et al.*, 2001; Vasseur & Gaedke, 2007; Keitt, 2008; Sheppard *et al.*, 2015) and matrix regressions and others (Haynes *et al.*, 2013). Many of the prior studies that have statistically illuminated the processes driving synchrony (e.g., Sheppard *et al.*, 2015; Shetakova *et al.*, 2016) have used temporally extensive data sets. Here, and following Defriez & Reuman (In review), we adopt a different approach, taking advantage of the unparalleled spatial coverage (but limited temporal extent) provided by remotely sensed data. We use data describing geographic patterns and variation in vegetation, globally, as measured through the enhanced vegetation index (EVI), process them so as to quantify and map the phenomenon of synchrony, and then make comparisons to geographic patterns in potential causal factors of synchrony. Drivers of synchrony should have statistically similar spatial patterns to the geographic patterns of synchrony revealed by the EVI data. We use spatial linear models to compare geographic patterns in EVI synchrony with putative drivers.

A key feature of several of the studies cited in the previous paragraph is their attention to the timescale dependence of population dynamics in synchrony, through the use of spectral methods. We also use spectral methods. Spectral methods allow the decomposition of synchrony into the frequencies, or timescales (timescale here indicating the reciprocal of frequency) at which it occurs, thereby showing which frequencies contribute most to synchrony. Synchrony on one timescale can be independent of synchrony on another timescale, and this independence can obscure analysis of synchrony by correlation based methods (Figure 1; Keitt, 2008; Sheppard

et al., 2015; Defriez *et al.*, 2016). In addition, synchrony on longer timescales may be more important than short-timescale synchrony because it is more likely to affect longer-lived consumers (Sheppard *et al.*, 2015; Defriez *et al.*, 2016). We believe timescale-specific approaches to synchrony are under-applied, and that this has limited our understanding of the causes and consequences of synchrony (Sheppard *et al.*, 2015; Defriez *et al.*, 2016).

Past researchers have typically considered Moran effects resulting from just one environmental driver at a time (Batchelder *et al.*, 2012; Sheppard *et al.*, 2015). However, it is possible, in principle, to have two or more distinct simultaneous Moran drivers of synchrony. These multiple Moran effects may, *a priori*, reinforce or counteract each other. Here we investigate the possibility that Moran effects from both land surface temperature and precipitation environmental drivers are simultaneously important for the synchrony of vegetation. We also include other possible covariates of synchrony: average EVI density (areas with more vegetation may, *a priori*, exhibit systematically more or less EVI synchrony), average temperature, average precipitation, average altitude, extent of variation in altitude, latitude, and average wind speed.

The main questions asked here are: Q1) What regions of the terrestrial realm exhibit high degrees of regional synchrony in vegetation density (as measured by EVI), and what areas exhibit low synchrony? Q2) When regional synchrony is decomposed into long- and short-timescale components, do maps differ in their main features, i.e., is the geography of synchrony timescale-specific? Q3) What are the main statistical determinants of synchrony in vegetation density, as inferred from its geography? Do determinants of long- and short-timescale synchrony differ? Q4) Do patterns of synchrony and statistical determinants of synchrony differ between major land masses? And finally Q5) Is there evidence for dual Moran effects contributing to synchrony in vegetation density? We hypothesize that: H1) Moran effects will be detectable via our approach, and will comprise some of the major determinants of vegetation synchrony and its

geography. Our past research (Sheppard *et al.*, 2015; Defriez *et al.*, 2016) indicates timescale-specific structure is a common feature of synchrony, so we also hypothesize that H2) Moran effects will be timescale-specific, and therefore the geography of synchrony will be timescale specific. H2 would be supported if short-timescale components of environmental synchrony are spatially associated with short- but not long-timescale components of vegetation synchrony, or if long-timescale components of environmental synchrony are spatially associated with long- but not short-timescale components of vegetation synchrony. This paper is the first explicit exploration we are aware of into the detailed geography of synchrony in terrestrial vegetation, and is also the first time the geography of synchrony has been used to infer determinants of synchrony in the terrestrial vegetation.

3 METHODS

3.1 Data

The Enhanced Vegetation Index (EVI) and land temperature emissivity data sets from the MODIS Aqua and Terra satellites were downloaded for the period 2001 to 2014 as C5 monthly products at a 0.05° resolution. 2014 was the last complete year available at the time the data were downloaded (September 2015). The EVI data products were retrieved from the online Data Pool, courtesy of the NASA Land Processes Distributed Active Archive Center (LP DAAC), USGS/Earth Resources Observation and Science (EROS) Center, Sioux Falls, South Dakota (`https://lpdaac.usgs.gov/data_access/data_pool`). EVI gives an indication of vegetation greenness and correlates well with gross primary productivity (Huete *et al.*, 2002; Sims *et al.*, 2015; Sjöström *et al.*, 2009). Compared to the Normalized Difference Vegetation

Index (NDVI) it minimizes the confounding effects of soil background, atmosphere and canopy density (Huete *et al.*, 1997, 2002; Xiao *et al.*, 2003). The pixels designated 'lowest quality' or below in the quality assurance flags and any estimated pixels (pixel reliability 4) were removed and the data were converted to 1° resolution by taking averages. Data from the Aqua and Terra satellites were averaged.

Daily precipitation values for the same time period were obtained from the Global Precipitation Climatology Project (GPCP) (Huffman *et al.*, 2001) as a 1° daily dataset compiled from satellite observations and rain gauge measurements. The daily precipitation data were averaged to monthly time series.

Annual time series for EVI, land surface temperature (LST) and precipitation were obtained from monthly time series for each 1° grid cell as long as there were no more than 5 missing months in an individual time series and no more than 1 missing month from any individual year. Otherwise the grid cell was omitted. Before annualising, missing months were replaced by the average value for that month for that time series. Time series were linearly detrended and their mean was subtracted before further analysis.

Altitude data were downloaded from the British Oceanographic Data Centre (`http://www.bodc.ac.uk/data/online_delivery/gebco/`) at one arc minute resolution. Data were re-gridded to 1° resolution by taking averages. Altitudes were log transformed due to a predominance of lower values. To account for the negative values of the few points on land below sea level, the minimum altitude was subtracted from all values and 1 was added before taking logs. The standard deviation of log-transformed altitude values over a 500km radius was also calculated for each cell.

Wind data were obtained from the National Centers for Environmental Prediction and the National Center for Atmospheric Research (NCEP/NCAR) reanalysis results provided by the National Oceanic and Atmospheric Administrations, Earth System Research Laboratory, Physical Science Division (`http://www.esrl.noaa.gov/psd/`; Kalnay *et al.* (1996)). Data were provided as velocity components, u representing the east-west component and v the north-south component of wind. Annual data were downloaded at 2.5° resolution over the time period 2001 to 2014 and were re-gridded to 1° resolution. Some 1° cells fell entirely within a 2.5° cell and were given the value of the larger cell. For 1° cells which crossed more than one 2.5° cell an average was taken. For each 1° cell an average of all annual values was calculated for the period of study. Wind speed was calculated from the u and v components with the formula $\sqrt{u^2+v^2}$. All datasets were downloaded September 2015.

3.2 Correlation-based synchrony

For EVI, temperature and precipitation (separately), for each 1° grid cell, Spearman's correlation was calculated between the annual time series of that focal cell and time series of each of the other cells within a 500 km radius. These values were averaged to produce a synchrony value for the focal cell. Global maps of the strength of synchrony (out to 500 km) were thereby produced for EVI, temperature and precipitation. These spatial variables will be referred to as *EVI synchrony*, *temperature/temp synchrony*, and *precipitation/precip synchrony* in subsequent spatial modeling. Because of the averaging over values for cells within 500 km of the focal cell, our synchrony maps are maps of regional synchrony. Justification for the specific choice of 500 km is in Appendix S1 in Supporting Information. We computed synchrony maps for distance bands 500-1000 km and 1000-1500 km to test sensitivity of patterns to the choice of distance band.

Spearman's correlation was used as not all time series were normally distributed and no single transformation was able to normalize all time series simultaneously.

3.3 High- and low-frequency synchrony

Following (Defriez *et al.*, 2016) a normalized cospectrum was used to decompose synchrony between time series according to the frequencies, or timescales, at which it occurred. The normalized cospectrum is the frequency specific decomposition of the correlation coefficient commonly used to the describe synchrony between two time series. It gives in-phase correlation between two time series as a function of frequency and, like the correlation coefficient, takes values between -1 and 1. So the input of the normalized cospectrum technique is two time series, and the output is a plot with x-axis showing frequency and y-axis showing in-phase synchrony between the time series at each frequency. Figure 1 gives idealized examples. An integral of the normalized cospectrum over all frequencies equals the correlation coefficient. The highest peaks in the normalized cospectrum correspond to frequency components that are most important in accounting for covariation in the time series.

To obtain the normalized cospectrum of two time series, one starts with their cospectrum (a standard method, see Brillinger, 2001), and normalizes by dividing by the geometric mean of the variances of the time series. Because the integral of the cospectrum of two time series is their covariance (Brillinger, 2001), this normalization ensures that the integral of the normalized cospectrum of the time series is their Pearson correlation coefficient. To make the integral equal the Spearman correlation used in the previous section, time series values were replaced by ranks prior to calculating the normalized cospectrum.

For EVI, temperature and precipitation (separately), for each 1° grid cell, normalized cospectra were calculated between the rank time series of that focal cell and the rank time series

of each other cell within 500km. The normalized cospectra were then integrated over 'high' (0.25-0.5 cycles/year) frequencies (timescales of 2 years to 4 years) and 'low' (0-0.25 cycles/year) frequencies (timescales exceeding 4 years) and average values for each frequency band within 500km were then computed. The resulting six spatial variables will be referred to as *high*- (respectively, *low*-) *frequency EVI synchrony*, *high*- (respectively, *low*-) *frequency temperature/temp synchrony*, and *high*- (respectively, *low*-) *frequency precipitation/precip synchrony*. Because the integral of the normalized cospectrum over the whole range of frequencies (0-0.5 cycles/year) equals the correlation, high- and low-frequency synchrony values for a cell for a given variable summed to the all-frequency values of the previous section. The terms *total* or *all-frequencies EVI/temp/precip synchrony* will sometimes be used to refer to the variables of the previous section, to specifically contrast them with frequency-specific quantities. Our use of the normalized cospectrum is described with formulas in Appendix S2, the dividing frequency 0.25 cycles/year is justified in Appendix S3, and a method is described in Appendix S4 for producing 95% confidence thresholds for values on maps of synchrony.

3.4 Statistical modeling

Spatial linear models were run with: 1) EVI synchrony as the response variable and temperature and/or precipitation synchrony potentially included as explanatory variables (among other potential explanatory variables, see below); and 2) high- and 3) low-frequency EVI synchrony as the response variable and high- and low-frequency temperature and precipitation synchrony potentially included (among others, see below) as explanatory variables instead of total temperature and precipitation synchrony. Total, high-, and low-frequency EVI synchrony were linearly mapped from the interval -1 to 1 onto the interval 0 to 1 and then logit transformed before models were run so that they were not limited by -1 and 1.

Four types of model were considered. First, standard linear models $y=X_1\beta+\varepsilon$ were considered, where y is the response variable (a column matrix with one entry for each grid cell for which data were available) and X_1 is the standard design matrix, with columns containing explanatory variables. The specific columns depended on the explanatory variables included in a given model (see below). Second, models with spatially "lagged" variables $y=X_1\beta+WX_2\delta+\varepsilon$ were considered (LeSage, 2014). If N is the number of grid cells for which data were available (this is the length of the column y) then W is an $N\times N$ matrix of weights encoding the geographic neighbourhoods of each location. The term $WX_2\delta$ represents neighbourhood, or spatially "lagged" effects of the explanatory variables in X_2 on the response variable, y, and the estimated parameters δ represent the strengths of these effects for each explanatory variable in X_2. Third, the spatial error model $y=X_1\beta+u$ was considered; and fourth, the spatial Durbin error model $y=X_1\beta+WX_2\delta+u$ (Elhorst, 2010) was considered, where for both models the equation $u=\lambda Wu+\varepsilon$ implicitly defines u, and u represents spatially autocorrelated residuals. See Appendix S5 for further details on the models.

Variables which could enter in a model are listed in abbreviation in table 1 and are explained here. Temporally averaged EVI (abbreviation 'EVI') in the focal cell, as well as temporally averaged land surface temperature ('temp') and precipitation ('precip') variables were used, as was average altitude within the focal cell (log transformed as described in the Data section, abbreviation 'log(altitude)'), standard deviation of log(altitude) values over grid cells within the 500 km radius disk centered at the focal cell ('sd log(altitude)') and average wind speed within a focal cell ('wind speed'). The strengths of synchrony of temperature and precipitation ('temp synchrony', 'precip synchrony'), as computed above, were also used to test for Moran effects.

Either total or low- and high-frequency versions of these variables were used, as described above. Variables could enter as local effects or, in models with lagged variables could enter as neighbourhood effects, the latter specified by 'lag' in table 1.

The variance inflation factor (VIF) was used to test for collinearity. VIF indicated only negligible collinearity among predictor variables (table S1 in Supporting Information), following the recommendations of Dormann *et al.* (2013) for assessing collinearity.

To limit the number of models fitted and because we sought main determinants of synchrony, the total number of variables allowed in any one model was restricted to 5 or fewer. For models with spatially lagged variables and for spatial Durbin error models, explanatory variables were allowed to enter the models either as part of X_1 (local effects) only, or as part of both X_1 and X_2 (both local and neighbourhood/lagged effects). Neighbourhood effects without local effects (i.e., putting a variable in X_2 but not X_1) were not considered.

For each model, the Bayesian information criterion (BIC) was calculated and BIC weights were computed to determine the top 95% confidence set of models. BIC was used instead of the Akaike information criterion (AIC) because it is known that AIC tends to favor more complex models (Burnham & Anderson, 2004) and we sought the main determinants of synchrony. Importance of a given variable as a predictor of EVI synchrony (total, low- or high-frequency) was measured by summing BIC weights across models that included the variable. Signs of model-averaged coefficients were computed (Burnham & Anderson, 2004). Residual plots were produced for top models to check that model assumptions were reasonable.

Spatial statistical models were fitted and model selection was performed using the global data. But if determinants of synchrony differed markedly by continent, the global analysis would represent an average of different processes. To diagnose whether important differences occurred

(Q4 from the Introduction), analyses were also run separately for Eurasia, Africa, North America, South America and Oceania. See Appendix S6 for methodological details.

BIC approaches can identify which of several models is best supported by the data (Burnham & Anderson, 2004), but do not, on their own, indicate whether any of the models was objectively good. We provided three pieces of information to assess model fit. First, we computed R^2, the fraction of spatial variation in EVI synchrony explained by the model. Second, we compared, via BIC and ANOVA, our best (lowest BIC) model from each model comparison exercise to the null model $y=X_1\beta+u$, for X_1 a column of 1s and u spatially autocorrelated residuals. All analyses were done using R v3.1.3. Spatial models were fitted using the R package spdep (Bivand & Piras, 2015).

4 Results

Figure 2a shows total EVI synchrony and answers Q1 from the Introduction by depicting which areas have relatively much and which areas have relatively little synchrony. The confidence threshold was very low compared to observed strengths of synchrony. The areas of highest synchrony are found in Africa over the Sahara and also in Botswana and Namibia. Eastern Brazil, Northern Europe and large areas of Australia were also highly synchronized. Regions of relatively low synchrony included areas on the west coast of South America, the Pacific Northwest of the United States, some islands of Oceania and areas in central China and West Africa. Global variation in the strength of synchrony was enormous, spanning essentially the entire range of possibilities from almost no synchrony (purple on Figure 2a) to almost perfect synchrony (yellow on Figure 2a). Patterns of synchrony were broadly similar for 500-1000km and 1000-1500km (Figure S1 in Supporting Information), but the geographic variation in strength

of synchrony at these distances was not as great, as may be expected because averages are computed across more space.

Answering Q2, geographic patterns of synchrony were strongly frequency specific (Figures 2c and 2d), with areas that were strongly synchronized at low frequencies often differing from (though sometimes being near to) areas that were strongly synchronized at high frequencies. For example, synchrony in the Sahara and in China predominantly occurred at low frequencies. Synchrony on the Atlantic coast of Brazil was primarily at low frequencies, but synchrony inland from the coast had a larger high-frequency component.

Both globally and for continental regions, spatial linear models of synchrony were fitted and ranked by BIC weight (tables S2-S7), variable importance tables were generated by summing BIC weights (tables 1, S8-S12), signs of model coefficients were tabulated (tables S13-S19) and model-averaged predictions were generated (Figure 2b, S2, S3). Figure 2b shows model-averaged total EVI synchrony as predicted by the top 95% confidence set of global models (by BIC weight). The models generally identified the areas of highest synchrony such as the Sahara, Southern Africa, and Eastern Brazil (compare to Figure 2a). However, predicted synchrony was often lower than observed synchrony when observed synchrony was high, and was higher than observed synchrony when observed synchrony was low: total geographic variation in the strength of synchrony was underestimated by the model. High synchrony in Northern Europe was also not captured by predictions. Although model predictions roughly captured large-scale trends, they were poor at representing fine spatial structure in synchrony. The best model explained 29% of the variation in total EVI synchrony (table S2). It had BIC far superior to the BIC of the null model $y=X_1\beta+u$, for X_1 a column of 1s: BIC was -626 for the best model, 307 for the null model. ANOVA revealed a highly significant difference between these models ($p<0.001$).

Models of frequency-specific synchrony explained less of the variation than models for all frequencies, as may be expected given the greater variability intrinsic to estimates of frequency-specific quantities (table S2). But BIC comparisons and ANOVA *p*-values nevertheless indicated highly meaningful differences between best models and the null model (Appendix S9).

Synchrony in temperature and precipitation are both consistently highly important in statistically explaining all-, high- and low-frequency EVI synchrony (table 1), answering Q3 from the Introduction. They have a positive effect, meaning greater synchrony in temperatures or precipitation is associated with greater synchrony in EVI, demonstrating the likely importance of Moran effects and supporting H1 from the Introduction. The importance of both variables supports the presence of dual Moran effects, answering Q5.

Results show that both temperature and precipitation effects are frequency specific, confirming H2 from the Introduction. High-frequency precipitation synchrony was a more important predictor of high-frequency EVI synchrony than it was of low-frequency EVI synchrony. Low-frequency temperature synchrony was a more important predictor of low-frequency EVI synchrony than it was of high-frequency EVI synchrony, and likewise for precipitation (table 1).

Given that both synchrony in temperature and synchrony in precipitation were important determinants of total EVI synchrony, it was possible, *a priori*, that interaction effects were present between the two. As there was only one supported model in the global, all-frequencies analysis (table S2) we compared that model to a model that had interaction effects between temperature and precipitation synchrony variables, but was otherwise the same. The BIC value of the model with interactions was -616 compared to -626 for the best model with no interactions, so there was no evidence for interaction effects.

Also important and also having a positive association with EVI synchrony were mean temperature and log altitude (table 1). These were important predictors for all frequencies and for high and low frequencies, separately. Average EVI itself was only an important predictor of high-frequency EVI synchrony, further demonstrating the frequency specificity of synchrony and its determinants.

Results for the continent-specific analyses (tables 2, S8-S12) were similar to global results, but with some heterogeneity in some determinants of synchrony, answering Q4 from the Introduction. Apparent dual Moran effects with temperature and precipitation drivers were supported at high, low, or all frequencies on all continents (table 2). The frequency-specificity of temperature effects is visible for all continents: either high-frequency temperature synchrony is only important for high-frequency EVI synchrony and not for low; or low-frequency temperature synchrony is only important for low-frequency EVI synchrony and not for high; or both (table 2). The same can be said for precipitation in Eurasia, Africa, and South America. Some of the variables not important in the global analysis were important when looking at specific continents (table 2, for all models see tables S3-S7). For example in Africa wind speed is an important determinant of synchrony across all and at low frequencies although it has opposite effects. At all frequencies it has a negative effect on EVI synchrony, but its lag has a positive effect, and at low frequencies it has a positive effect. Mean EVI itself is also important at all frequencies for two continents, South America and Oceania; and at high frequencies for three, Africa and South and North America. It always has a positive effect: areas with higher EVI values have greater EVI synchrony. In continent-specific analyses, best models were always much better than the null model ($y=X_1\beta+u$, for X_1 a column of 1s) according to BIC comparisons and ANOVA results (Appendix S9).

5 Discussion

Our principle result is that there is an important geography of synchrony of terrestrial vegetation, globally. Regional (500 km) synchrony varied enormously, from areas with almost no synchrony to areas with near-perfect synchrony. Dual apparent Moran effects of precipitation and temperature were the major statistical determinants of EVI synchrony and its geographic patterns worldwide, with some variation among continents in the details of these effects and in the importance of other determinants of synchrony. The geography and determinants of synchrony were strongly frequency specific. Inferences leading to our conclusions about likely Moran effects and frequency-specificity of synchrony were effective because they exploited the geography of synchrony. Moran effects from a single environmental driver have been reported (e.g., Batchelder *et al.*, 2012; Sheppard *et al.*, 2015), and studies have combined multiple drivers using PCA (Haynes *et al.*, 2013). However, as far as we are aware, this is the first or one of few studies to provide evidence for two distinct separate synchronous environmental variables driving ecological synchrony in concert. Additional observations on effects of altitude on synchrony and the partial coincidence of high-synchrony areas with arid regions are in Appendix S7.

This work complements Defriez & Reuman (In review), in which we analyzed the main statistical determinants of synchrony in ocean chlorophyll. The key similarities between synchronies of chlorophyll and terrestrial vegetation are that the geography of synchrony was pronounced in both contexts, and Moran effects were statistically supported and frequency specific. There were also differences. Chlorophyll synchrony is highest in areas where chlorophyll itself is low; but EVI often has a positive association with EVI synchrony.

It is well known that temperature and precipitation can be important factors in vegetation dynamics (Ichii *et al.*, 2002; Piao *et al.*, 2006; Clinton *et al.*, 2014). However, our new result that

geographies of synchrony in temperature and precipitation are important correlates of the geography of EVI synchrony, while true, does not follow automatically from the earlier knowledge. Defriez & Reuman (In review) found that the geography of synchrony of incident solar irradiance was not statistically related to the geography of synchrony in chlorophyll-*a* abundance in the world's oceans, even though it is well known that irradiance can be an important factor in chlorophyll-*a* dynamics. In complex ecosystems, known importance of an environmental factor for ecological dynamics does not necessarily mean the factor produces a Moran effect or a geography of synchrony, for several potential reasons, including: the possibility that the environmental factor itself has a muted geography of synchrony; and the possibility that the factor's influence on vegetation is nonlinear or complex in some important way that varies geographically (see, e.g., Defriez & Reuman, In review, where mechanisms are discussed for the phytoplankton case). The following paragraphs explore some of these complexities further.

Non-monotonic relationships are increasingly important in ecology (Zhang *et al.*, 2015). A non-monotonic effect of an environmental variable on a population variable may modify the extents to which Moran effects can occur and the geographies of synchrony of the environmental and population variables match. To illustrate the concept, suppose the population $p_i(t)$ at time t in location i, for i=1,2, equals $f(e_i(t))$ for $e_i(t)$ some environmental variable. And suppose f is an increasing function of e_i for $e_i<o$ and decreases for $e_i>o$. Then even if $e_1(t)$ and $e_2(t)$ are perfectly synchronous through time, the populations $p_i(t)$ need not be perfectly synchronous. For instance, if the mean of e_i is less than o for i=1 and greater than o for i=2, many year-to-year fluctuations in the environment will produce opposite effects in the two populations. For more than two locations, geographic variation in local mean environments could produce a geography of population synchrony even if the environmental fluctuations are perfectly correlated across all

locations. Although this example is oversimplified, it illustrates that non-monotonicity may mediate relationships between the geographies of synchrony of population variables and their environmental drivers. Our methods probably cannot illuminate intricacies such as these, if they are indeed important in real systems. These ideas may reveal a worthwhile area for future research.

The carrying capacity of vegetation varies globally due to spatial variation in soils and other factors, and therefore the nature of density dependence in vegetation dynamics also varies spatially. Liebhold *et al.* (2006) describe a reduction in environmentally caused spatial synchrony resulting from geographic variation in density dependent dynamics. The effect can mediate or produce a geography of population synchrony, and is related to the concepts of the previous paragraph. If spatial variation in density dependence over a region is pronounced, the geography of ecological synchrony need not match the geography of synchrony of an environmental driver.

Although temperature and precipitation are key drivers of primary productivity, which of these is more important can differ among biomes (Nemani *et al.*, 2015). For example, precipitation is often found to be more tightly coupled with vegetation and productivity in arid zones (Zhang, 2005; Fabricante *et al.*, 2009). Although it is difficult to tell from the analyses of this study whether both synchrony in temperature and synchrony in precipitation are driving EVI synchrony everywhere across a given continent or if their relative importance varies, future work might be able to illuminate this question. There is substantial heterogeneity globally in the correlation between EVI and precipitation and temperature intra-annually (Clinton *et al.*, 2014). Furthermore, in Africa, according to our results, there are two areas of strong synchrony: the Sahara and an area in Southern Africa. Synchrony in the Sahara is predominantly at low frequencies (Figure 2d) whereas synchrony in Southern Africa is predominantly at high frequencies (Figure 2c). Both high-frequency precipitation synchrony and high-frequency

temperature synchrony were important determinants of high-frequency EVI synchrony in Africa; but only low-frequency temperature synchrony, and not low-frequency precipitation synchrony, was an important determinant of low-frequency EVI synchrony. This suggests that in Southern Africa synchrony in both temperature and precipitation drive synchrony in vegetation density but in the Sahara only synchrony in temperature drives synchrony in vegetation density, despite the tight coupling with precipitation often found in arid regions (Zhang, 2005; Fabricante *et al.*, 2009). The wavelet methods of Sheppard *et al.* (2015) can illuminate what is causing synchrony with no need to rely on geographic variation in synchrony. Although our time series are probably too short for their wavelet analyses, a Fourier version of the techniques of Sheppard *et al.* (2015), applied separately to different regions of Africa (and elsewhere) might identify precisely how temperature and precipitation trade off against each other in relative importance as Moran drivers.

We used land surface temperatures (LST) as opposed to surface air temperatures (SAT, measured at 1.5-2m above ground level) because LST is available from satellite measurements and SAT is measured at discrete weather stations. Data products that provide SAT estimates globally based on interpolation between weather stations are available, but interpolation creates artefactual synchrony, so those products could not be used. LST can be affected by vegetation cover and condition (through evapotranspiration), and by soil wetness and therefore precipitation (Jin & Dickinson, 2010; Mildrexler *et al.*, 2011), so causal relationships between our temperature and EVI synchrony variables may be complex and are incompletely illuminated by our correlative statistical approach. It is possible that temperature synchrony causes EVI synchrony through Moran effects, or that EVI synchrony causes temperature synchrony through vegetation effects on LST, or, most probably in our opinion, that the factors jointly affect each other or the causal relationship itself varies geographically. Our models establish statistical determinants of synchrony, a necessary but not sufficient condition for a causal effect of temperature synchrony

on EVI synchrony. SAT may be a better variable for improving causal understanding of synchrony in future research, though a modified statistical approach would be needed to account for the fact that direct SAT measurements are only available at weather stations.

Changes in synchrony through time have received recent attention (Sheppard *et al.*, 2015; Defriez *et al.*, 2016; Shetakova *et al.*, 2016; Koenig & Liebhold, 2016), raising the possibility of changes in synchrony superimposed on the geography of synchrony or affecting this geography itself. Shetakova *et al.* (2016) describe increasing synchrony through time in spatio-temporal forest tree growth data. They concluded that observed increases are not due to increasing synchrony of Moran drivers, but instead to stronger synchronizing influence of the drivers: as climate becomes more extreme and impacts in climatic variation therefore become more widely influential on ecosystems, climate has a more synchronizing influence even when climate need not itself have become more spatially synchronous. In our analysis we did not address the possibility of changes in synchrony with the passage of time - our time series are probably too short to do so. Although we removed trends before calculating synchrony we found mean temperature was an important determinant of synchrony across all frequencies, and has a positive effect. The results of Shetakova *et al.* (2016) raise the possibility that longer term increases (or decreases) in synchrony may be superimposed on top of the spatial patterns we found. Changes in synchrony may also interact with and modify spatial patterns of synchrony. To examine this possibility one would need data that are extensive both spatially and temporally. Synchrony is ecologically important, as metapopulations displaying increased spatial synchrony have an increased risk of extinction (Heino *et al.*, 1997). It has also been proposed that an increase in spatial correlation may occur in environments before a regime shift (Dakos *et al.*, 2010). As such, our study may act as a baseline for examining future changes in synchrony and its geography, in addition to being one of the first to document the geography of synchrony at all.

6 Acknowledgments

We thank LW Sheppard, J Walter, TL Anderson, L Zhao, G Karki, D Orme, A Purvis, S Jennings, and G Woodward for helpful discussions and comments and for statistical advice. ED was supported and DCR was partly supported by United Kingdom Natural Environment Research Council grants NE/H020705/1, NE/I010963/1, NE/I011889/1. DCR was partly supported by the James S McDonnell Foundation, by the University of Kansas tier II strategic research fund and general research fund, and by NSF grant 1442595. Travel was facilitated by US National Science Foundation grant DMS-1225529.

Data underpinning this work is available freely online at locations indicated within the methods. The date data were downloaded for this work is also indicated within the methods.

7 Supporting Information Short Captions

S1) Justification for 500 km disks: On the choice to use 500 km disks.

S2) The normalized cospectrum: Some details of the method.

S3) Dividing frequency between low and high: Why 0.25 was used.

S4) Confidence thresholds on synchrony maps: Details of the method.

S5) Details of spatial statistics: Details of the method.

S6) Continent-specific models: Details of the methods.

S7) Observations on altitude and arid regions: Discussion points.

S8) Supporting results: Including results from individual continents.

S9) Plots of model residuals: Residual plots for top models.

8 BIOSKETCH

Emma Defriez and Daniel Reuman are ecologists with interests in spatio-temporal patterns of population dynamics and how these are affected by environmental processes at different scales.

9 REFERENCES

Abbott K (2007) Does the pattern of population synchrony through space reveal if the moran effect is acting? *Oikos*, **116**, 903–912.

Batchelder HP, Mackas DL, O'Brien TD (2012) Spatial-temporal scales of synchrony in marine zooplankton biomass and abundance patterns: A world-wide comparison. *Progress in Oceanography*, **97**, 15–30.

Beer C, Reichstein M, Tomelleri E, *et al.* (2010) Terrestrial gross carbon dioxide uptake: Global distribution and covariation with climate. *Science*, **329**, 834–838. 10.1126/science.1184984.

Bivand R, Piras G (2015) Comparing implementations of estimation methods for spatial econometrics. *Journal of Statistical Software*, **63**, 1–36. URL `http://www.jstatsoft.org/v63/i18/`.

Bjørnstad ON, Falck W (2001) Nonparametric spatial covariance functions: Estimation and testing. *Environmental and Ecological Statistics*, **8**, 53–70.

Brillinger D (2001) *Time Series: Data Analysis and Theory*. Society for Industrial and Applied Mathematics, Philadelphia.

Burnham KP, Anderson DR (2004) Multimodal interference: Understanding AIC and BIC in model selection. *Sociological Methods and Research*, **33**, 261–304.

Clinton N, Yu L, Fu H, He C, Gong P (2014) Global-scale associations of vegetation phenology with rainfall and temperature at a high spatio-temporal resolution. *Remote Sensing*, **6**, 7320–7338.

Dakos V, van Nes EH, Donangelo R, Fort H, Sheffer M (2010) Spatial correlation as leading indicator of catastrophic shifts. *Theoretical Ecology*, **3**, 163–174.

Defriez EJ, Reuman DC (In review) A global biogeography of synchrony for marine phytoplankton. *In Review*.

Defriez EJ, Sheppard LW, Reid PC, Reuman DC (2016) Climate change-related regime shifts have altered spatial synchrony of plankton dynamics in the north sea. *Global Change Biology*. doi:10.1111/gcb.13229.

Dormann C, Elith J, Bacher S, *et al.* (2013) Collinearity: a review of methods to deal with it and a simulation study evaluating their performance. *Ecography*, **36**, 27–46.

Elhorst JP (2010) Applied spatial econometrics: Raising the bar. *Spatial Economic Analysis*, **5**, 9–28.

Fabricante I, Oesterheld M, Paruelo JM (2009) Annual and seasonal variation of ndvi explained by current and previous precipitation across northern patagonia. *Journal of Arid Environments*, **73**, 45–753.

Grenfell BT, Bjørnstad ON, Kappey J (2001) Travelling waves and spatial hierarchies in measles epidemics. *Nature*, **414**, 716–723.

Hanski I, Woiwod IP (1993) Spatial synchrony in the dynamics of moth and aphid populations. *Journal of Animal Ecology*, **62**, 656–668.

Haynes KJ, Bjørnstad ON, Allstadt AJ, Liebhold AM (2013) Geographical variation in the spatial synchrony of a forest-defoliating insect: isolation of environmental and spatial drivers. *Proceedings of the Royal Society of London Series B- Biological Sciences*, **280**, 2012–2373.

Heino M, Kaitala V, Ranta E, Lindstrom J (1997) Synchronous dynamics and rates of extinction in spatially structured populations. *Proceedings of the Royal Society of London Series B-Biological Sciences*, **264**, 481–486.

Huete A, Didan K, Miura T, Rodriguez EP, Gao X, Ferreira LG (2002) Overview of the radiometric and biophysical performance of the modis vegetation indices. *Remote Sensing of Environment*, **83**, 195–213.

Huete AR, Liu HQ, van Leeuwen W (1997) A comparison of vegetation indices over a global set of tm images for eos-modis. *Remote Sensing of Environment*, **59**, 440–451.

Huffman GJ, Adler RF, Morrissey M, *et al.* (2001) Global precipitation at one-degree daily resolution from multi-satellite observations. *Journal of Hydrometeorology*, **2**, 32–50.

Ichii K, Kawabata A, Yamaguchi Y (2002) Global correlation analysis for NDVI and climatic variables and NDVI trends: 1982-1990. *International Journal of Remote Sensing*, **23**, 3873–3878.

Jin M, Dickinson RE (2010) Land surface skin temperature climatology: benefitting from the strengths of satellite observations. *Environmental Research Letters*, **5**, 044004. doi:10.1088/1748-9326/5/4/044004.

Kalnay E, Kanamitsu M, Kistler R, *et al.* (1996) The ncep/ncar 40 year reanalysis project. *Bulletin of the American Meteorological Society*, **79**, 2753–2769.

Keitt TH (2008) Coherent ecological dynamics induced by large-scale disturbance. *Nature*, **454**, 331–334.

Koenig WD (2002) Global patterns of environmental synchrony and the moran effect. *Ecography*, **25**, 283–288.

Koenig WD, Liebhold AM (2016) Temporally increasing spatial synchrony of North American temperature and bird populations. *Nature Climate Change*. doi: 10.1038/NCLIMATE2933.

Lande R, Engen S, Saether BE (1999) Spatial scale of population synchrony: environmental correlation versus dispersal and density regulation. *American Naturalist*, **154**, 271–281.

LeSage JP (2014) What regional scientists need to know about spatial econometrics. *The Review of Regional Studies*, **44**, 13–32.

Liebhold A, Johnson DM, Bjørnstad ON (2006) Geographic variation in density-dependent dynamics impactsthe synchronizing effect of dispersal and regional stochasticity. *Population Ecology*, **48**, 131–138.

Liebhold A, Koenig WD, Bjørnstad ON (2004) Spatial synchrony in population dynamics. *Annual Review of Ecology, Evolution, and Systematics*, **35**, 467–490.

Meir P, Coxon P, Grace J (2006) The influence of terrestrial ecosystems on climate. *Trends in Ecology and Evolution*, **21**, 254–260.

Mildrexler DJ, Zhao M, Running SW (2011) A global comparison between station air temperatures and modis land surface temperatures reveals the cooling role of forests. *Journal of Geophysical Research*, **116**. doi:10.1029/2010JG001486.

Moran PAP (1953) The statistical analysis of the canadian lynx cycle. ii. synchronization and meteorology. *Australian Journal of Zoology*, **1**, 291–298.

Myers RA, Mertz G, Bridson J (1997) Spatial scales of interannual recruitment variations of marine, anadromous, and freshwater fish. *Canadian Journal of Fisheries and Aquatic Sciences*, **54**, 1400–1407.

Nemani RR, Keeling CD, Hashimoto H, *et al.* (2015) Climate-driven increases in global terrestrial net primary production from 1982 to 1999. *Science*, **300**, 1560–1563.

Piao S, Fang J, Wei J, Guo Q, Ke J, Tao S (2006) Variation in a satellite-based vegetation index in relation to climate in china. *Journal of Vegetation Science*, **15**, 219–226.

Post E, Forchhammer MC (2004) Spatial synchrony of local populations has increased in association with the recent northern hemisphere climate trend. *Proceedings of the National Academy of Sciences of the United States of America*, **101**, 9286–90.

Ranta E, Kaitala V, Lindstrom J (1999) Spatially autocorrelated disturbances and patterns in population synchrony. *Proceedings of the Royal Society of London Series B-Biological Sciences*, **266**, 1851–1856.

Sheppard L, Bell J, Harrington R, Reuman DC (2015) Changes in large-scale climate alter spatial synchrony of aphid pests. *Nature Climate Change*, **6**, 610–613. doi:10.1038/nclimate2881.

Shetakova TA, Guiérrez E, Kirdyanov AV, *et al.* (2016) Forests synchronize their growth in contrasting eurasian regions in response to climate warming. *Proceedings of the National Academy of Sciences of the United States of America*, **113**, 662–667.

Sims D A Rahman AF, Cordova VD, El-Masri BZ, *et al.* (2015) On the use of modis evi to assess gross primary productivity of north american ecosystems. *Journal of Geophysical Research*, **111**. 10.1029/2006JG000162.

Sjöström M, Ardö J, Eklundh L, *et al.* (2009) Evaluation of satellite based indices for gross primary production estimates in a space savanna in the sudan. *Biogeosciences*, **6**, 129–138.

Vasseur DA, Gaedke U (2007) Spectral analysis unmasks synchronous and compensatory dynamics in plankton communities. *Ecology*, **88**, 2058–2071.

Wieder W, Cleveland C, Smith W, Todd-Brown K (2015) Future productivity and carbon storage limited by terrestrial nutrient availability. *Nature Geoscience*, **8**, 441–444.

Xiao BB, Zhang Q, Boles S, Frolking S, Moore B (2003) Sensitivity of vegetation indices to atmospheric aerosols: Continental-scale observations in northern asia. *Remote Sensing of Environment*, **84**, 385–392.

Zhang X (2005) Monitoring the response of vegetation phenology to precipitation in africa by coupling modis and trmm instruments. *Journal of Geophysical Research: Atmosphere*, **110**. doi:10.1029/2004JD005263.

Zhang Z, Yan C, Krebs C, Stenseth N (2015) Ecological non-monotonicity and its effects on complexity and stability of populations, communities and ecosystems. *Ecological Modelling*, **312**, 374–384.

Zhu Z, Piao S, Myneni RB, *et al.* (2016) Greening of the earth and its drivers. *Nature Climate Change*, **6**, 791–795. doi:10.1038/nclimate3004.

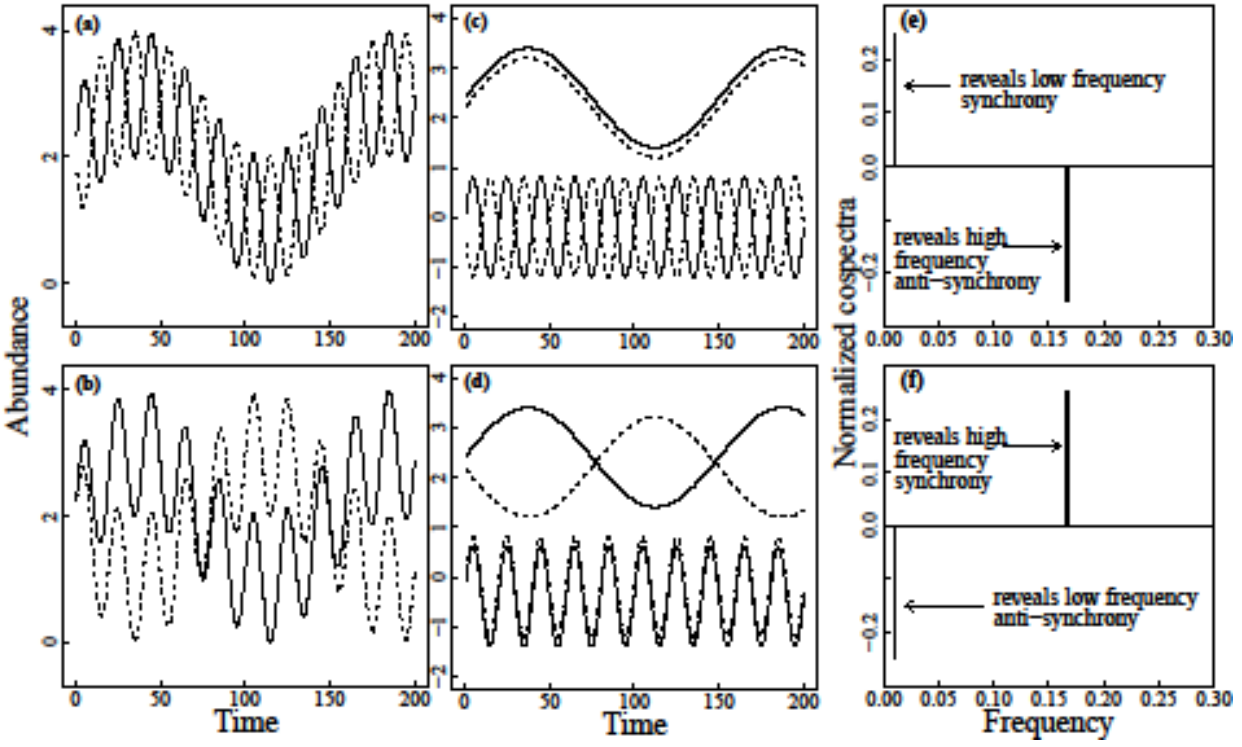

Figure 1: Idealized illustration of how synchrony can differ by timescale. (a) Time series are synchronous on long and anti-synchronous on short timescales. (b) Time series are anti-synchronous on long and synchronous on short timescales. (c, d) Decomposition to the individual frequencies that sum to form the time series in a and b, respectively. Standard correlation coefficients between time series are 0 for both (a) and (b), misleadingly suggesting lack of important synchronous phenomena. Note that normalized cospectra (e, f; Methods) reveal that positive synchrony at one frequency is masked by negative synchrony at the other. In practice, exact cancellation is unlikely. But asynchrony at some frequencies may nevertheless strongly conceal important synchrony at other frequencies. This figure is reproduced from Defriez *et al.* (2016).

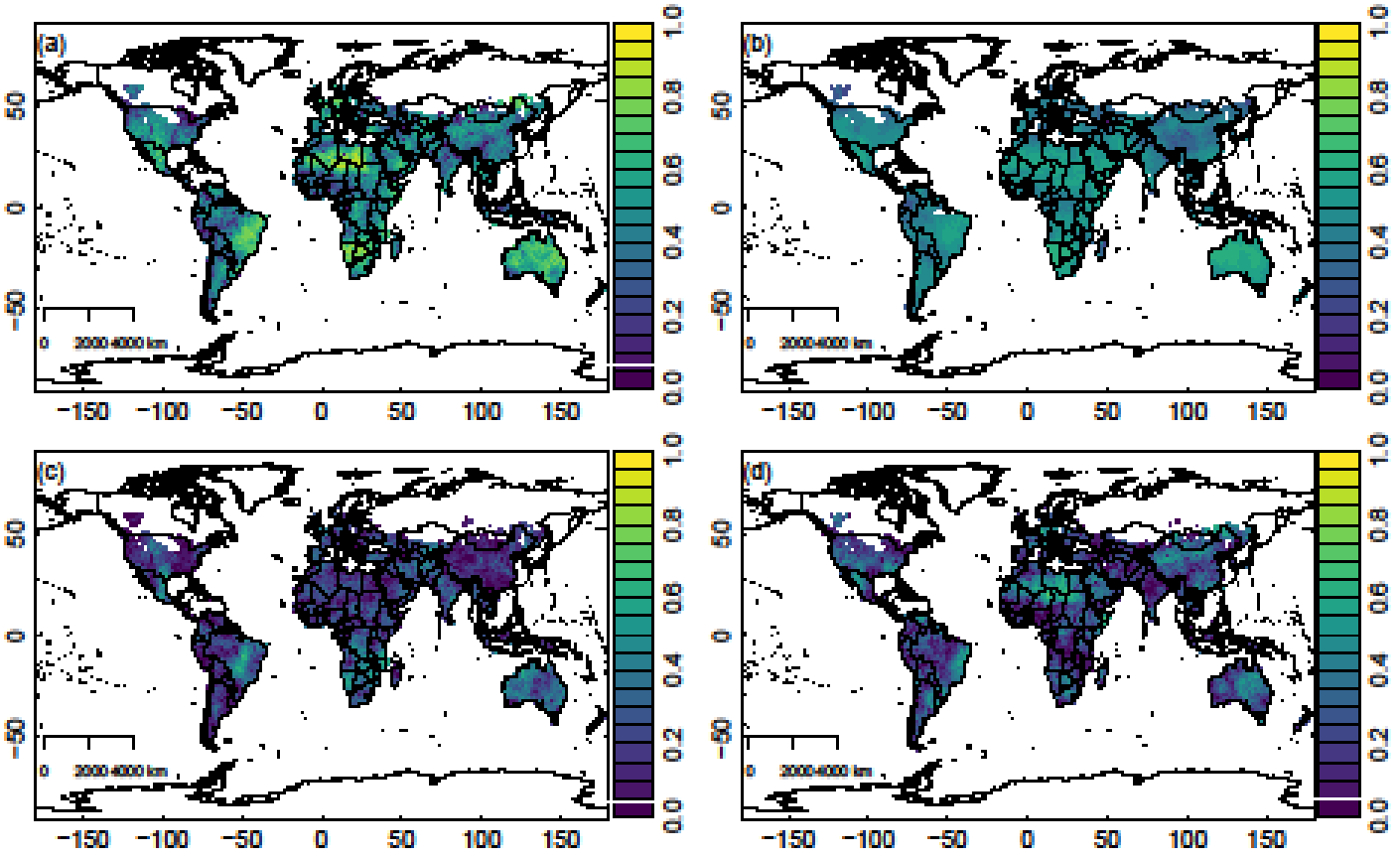

Figure 2: a) Observed EVI synchrony, all frequencies. b) Predicted EVI synchrony, all frequencies, from the 95% confidence set of models. c) Observed high-frequency EVI synchrony (timescales of 2-4 years). d) Observed low-frequency synchrony (timescales exceeding 4 years). The white horizontal lines on the colour legends in a, c, d are approximate 95% significance thresholds compared to a null hypothesis of no synchrony (Appendix S4). Projection is equidistant cylindrical.

	All Frequencies	+/-	High	+/-	Low	+/-
EVI	0.00888	+	**1.00000**	+	0.00000	-
EVI lag	0.00000	-	0.00000	-	0.00000	-
temp	**1.00000**	+	**1.00000**	+	**1.00000**	+
temp lag	0.00000	-	0.00000	-	0.00000	+
temp synchrony	**1.00000**	+				
temp synchrony lag	0.00800	+				
temp synchrony high			**1.00000**	+	**0.99991**	+
temp synchrony high lag			0.00000	+	0.00000	+
temp synchrony low			0.00046	+	**1.00000**	+
temp synchrony low lag			0.00000	-	0.00013	+
precip	0.00002	-	0.00000	-	0.00001	-
precip lag	0.00000	-	0.00000	-	0.00000	-
precip synchrony	**0.99192**	+				
precip synchrony lag	**0.99099**	+				
precip synchrony high			**0.99950**	+	0.00001	-
precip synchrony high lag			0.13876	+	0.00000	-
precip synchrony low			0.00000	-	**0.99999**	+
precip synchrony low lag			0.00000	-	0.00894	+
log(altitude)	**1.00000**	+	**0.86123**	+	**0.99098**	+
log(altitude) lag	0.00000	-	0.00000	-	0.00000	-
sd log(altitude)	0.00000	-	0.00002	-	0.00000	-
sd log(altitude) lag	0.00000	+	0.00000	+	0.00000	+
abs(latitude)	0.00019	+	0.00000	+	0.00003	+
wind speed	0.00000	+	0.00000	+	0.00000	+
wind speed lag	0.00000	+	0.00000	+	0.00000	+

Table 1: Variable importance as shown by sums of BIC weights of models that contain each variable (Burnham & Anderson, 2004), for global data. Values are between 0 and 1, larger values correspond to more important predictors. + or - indicate whether model-averaged coefficients of each variable are positive or negative. Variables in bold indicate those that are meaningfully high (their summed BIC weight was greater than or equal to 0.6). The abbreviations temp and precip stand for temperature and precipitation respectively, and “lag" indicates a variable entering as a spatially lagged, neighbourhood effect (Methods). Columns give results of separate spatial statistical analyses of total, high-frequency, and low-frequency synchrony maps.

Eurasia	+/-	Africa	+/-	NAmerica	+/-	SAmerica	+/-	Oceania	+/-
All Frequencies									
temp	+	temp synchrony	+	temp	+	EVI	+	EVI	+
temp synchrony	+	temp synchrony lag	+	temp synchrony	+	temp	+	temp	+
log(altitude)	+	log(altitude)	+	precip	+	temp synchrony	+	temp synchrony	+
abs(latitude)	+	wind speed	-	precip lag	-	log(altitude)	+	log(altitude)	+
		wind speed lag	+					log(altitude) lag	-
High Frequencies									
temp	+	EVI	+	EVI	+	EVI	+	temp	+
temp synchrony high	+	temp	+	temp synchrony high	+	temp	+	temp synchrony high	+
precip synchrony high	+	temp synchrony high	+	sd log(altitude)	-	temp synchrony high	+	log(altitude)	+
precip synchrony high lag	+	precip synchrony high	+			temp synchrony high lag	+	log(altitude) lag	-
		log(altitude)	+						
Low Frequencies									
temp synchrony high	+	temp synchrony low	+	temp	+	temp synchrony low	+	temp synchrony high	+
temp synchrony low	+	wind speed	+	precip synchrony high	+	precip synchrony low	+	temp synchrony low	+
precip synchrony low	+			precip synchrony low	+	precip synchrony low lag	+	precip synchrony high	-

Table 2: Most important variables driving EVI synchrony by continent. Variables were included if their summed BIC weight was greater than or equal to 0.6. The + or - signs indicate whether model-averaged coefficients of each variable are positive or negative.